Available online at www.sciencedirect.com
SCIENCE DIRECT®
Pergamon
Cement and Concrete Research 34 (2004) 1131–1143
CEMENT AND CONCRETE RESEARCH

Triaxial mechanical behaviour of mortar: Effects of drying

Ismail Yurtdas[a,b,c], Nicolas Burlion[a,c,*], Frédéric Skoczylas[a,b]

[a]Laboratory of Mechanics of Lille, UMR CNRS 8107, USTL, France
[b]Ecole Centrale de Lille, Cité Scientifique, 59650 Villeneuve d'Ascq, France
[c]Polytech'Lille-USTL, Cité Scientifique, 59650 Villeneuve d'Ascq, France

Received 21 November 2002; accepted 1 December 2003

Abstract

The analysis of concrete structure durability is based on the investigation of the material long-term behaviour. Such behaviour is influenced by mechanical, hydrous and thermal actions applied to structures. The main purpose of this study concerns the characterisation of the coupled effects between drying shrinkage and damage for a cementitious material. An experimental study on a normalised mortar (European norm) is then presented to characterise the damage effect, induced by drying and desiccation shrinkage on the multiaxial compressive behaviour. Triaxial compression tests are carried out at different times of drying. The observed increase in deviatoric strength and decrease of Young's modulus and Poisson's ratio are related to the loss in mass of specimens. These results are commented through the damage processes of material because the drying phenomenon causes microcracking by exceeding tensile strength. This microcracking will have a strong influence on the damage process of the material and then on its failure behaviour. Furthermore, the effect of drying leads to an increase of the capillary suction into the mortar, hence, to an increase of the specimen strength. Such couplings have to be taken into account in a reliable modelling.

Keywords: Triaxial mechanical behaviour; Mortar; Drying; Desiccation shrinkage; Coupling

1. Introduction

Cementitious materials are commonly subjected to multiaxial mechanical loading when these are used, for example, in nuclear power plant, prestress concrete, or when the impact of a missile on concrete structure has to be studied [1]. The understanding and the economic use [2,3] of these materials require the knowledge of its behaviour under multiaxial stresses, in particular, under axisymmetric triaxial compression. Until now, numerous studies were led to know the behaviour of concretes and mortars, and to model them under triaxial compression [1–9], that is, only under mechanical stresses. Moreover, these materials must be durable in time, in other words, to ensure long lifetime properties to face damages such as hydrous microcracking, chemical attack and physical damages. Coupling these various mechanisms makes more difficult for the elaboration of predictive and reliable modelling on one hand, and requires a very complete experimental study for the identification of the relevant parameters on the other hand.

We have thus studied, in our laboratory, the coupling "triaxial compression behaviour-desiccation shrinkage" for a mortar having a water by cement ratio equal to 0.5. Only few data can be found in the literature upon the influence of the drying shrinkage on the multiaxial behaviour of cementious materials under confining pressure, while numerous results on strains due to different kind of shrinkages are available. The present work puts in light that studying this coupling, for a predictive and reliable modelling, is crucial as the elastic parameters and the strength of the material show significant variations. Moreover, the mechanical behaviour of a cementitious material under triaxial compression is sensitive to the variation of its internal humidity [10–12] and to the applied confinement level [1–7,9,13]. Furthermore, Bažant and Raftschöl [14] showed that to avoid any cracking during drying, it was necessary to vary the relative surrounding humidity slowly and gradually, resulting to relative humidity differences inside the specimen lower than 2%, and to use test specimen of unusual

* Corresponding author.
E-mail address: Nicolas.Burlion@polytech-lille.fr (N. Burlion).

0008-8846/$ – see front matter © 2003 Elsevier Ltd. All rights reserved.
doi:10.1016/j.cemconres.2003.12.004

thickness (about 1 mm). Uniform drying is going with an increase in capillary pressure, surface tensions or disjoining pressures, which play an important role because the mechanical behaviour of material during its drying has to be identified. Furthermore, matrix deformations are prevented by aggregates leading to a diffuse cracking in cement paste [15–19]. While considering structures, geometrical effects induce a non-uniform distribution of relative humidity, even if the drying process is extremely slow. If they are suddenly exposed to external relative humidity variations, only 0.1-mm thickness structures would be exempt of microcracks. That means that heterogeneous drying microcracking may take place [14,15,20], even if no mechanical load is applied. In a general case, strains induced by hydrous gradient are prevented by structural effect; as a result, the cementing matrix is subjected to tensile stresses, which induce microcracks if tensile strength is exceeded. Thus, induced cracking due to these effects (material and structural) will have an influence on elastic properties, damaging process and failure stress of material [12,21,22].

Besides the drying process, the material behaviour is also very sensitive to the confining pressure as, when the latter is increased, a transition—brittle to ductile—can be observed [1–3,6,23]. Under a low confining level, rupture of concrete occurs with significant microcracking [2,3], while under high confining pressure, the failure takes place with slight microcracking [2,3] and major macrocracks, which separate the sample in two or three parts [1]. The confining pressure increase also changes the orientation of the rupture plan [5]. For very high confinement (up to 100 MPa), mechanical concrete behaviour becomes stiffening [24]. Hence, the possible influence of the induced microcracking and desiccation shrinkage upon the behaviour under low confinement and the failure process will be one of the main objectives of this study, as well as the induced capillary pressure effects.

In the first part, the setting up of the experimental program and the necessary requirements (the studied material and the experimental process) are described. In the second part, the obtained results are presented to underline the mechanical behaviour evolution of a mortar, under hydrostatic and triaxial compression stresses, in relation with the drying process. These results are analysed by putting forward the coupling effects between drying shrinkage and the multiaxial mechanical behaviour.

2. Elaboration of the experimental program

Total shrinkage of mortar and concrete comes from several shrinkages [21,25]: endogenous (including "Le Châtelier" contraction and self-desiccation shrinkage), thermal and desiccation shrinkage, which is the object of this study. Further shrinkage, known as carbonation shrinkage, can take place for samples preserved, during a long period of time, in a highly charged atmosphere with CO_2 [23,26]. Drying shrinkage was assumed to have prevailed within the present study, thus, carbonation shrinkage, supposed to be negligible, was not measured. The main cause of inducing drying shrinkage is commonly assumed to be the loss of free water [12,21]. Thus, hydrous gradient takes place from the heart to external sides of the sample, which, coupled with a low material permeability, will cause a differential drying shrinkage, leading to tensile stresses at the outer surface. As a result, there is initiation and propagation of microcracks, whether tensile strength is exceeded. In parallel, the cementing matrix contraction will arise around the aggregates, which are there like rigid inclusions. From this, a diffuse cracking may result depending on aggregate sizes [17–19]. In this work, the influences of the drying shrinkage on the damageable elastic-plastic behaviour of a mortar were studied using triaxial compression tests. For that purpose, a particular experimental procedure was designed.

2.1. Composition of mortar and samples conservation

To carry out this study, a normalised mortar of classical composition (see Table 1) was used and compound with a normalised sand (European norm EN196-1) and an often used cement. Such mortar has the advantage to be easily reproduced by other laboratories.

The necessary amount of mortar to achieve the whole study was cast at the same time in a beam formwork (4-m length, 150×150 mm^2 section), whose surface in contact with room atmosphere [temperature (T)=21 ± 1 °C, relative humidity (Hr)=60 ± 5%] was protected by a plastic cover to prevent a local desiccation. Five days later, the beam was immerged for 6 months in water regulated at 20 °C. At the end of this period, effects of thermal and endogenous shrinkages are thus negligible, while maturation of mortar is almost achieved. Samples used for the mechanical tests (37-mm diameter, 74-mm length) and for the permeability and porosity measurements (37-mm diameter, 90-mm length) were cored and cut from the beam, then carefully rectified to obtain a perfect geometry. Sample dimensions were chosen to measure the relevant parameters within a reasonable period of time. Let us note that cylinders used for transport property measurements (90-mm length) were cut in three parts: a central one of 50 mm intended for permeability measures, two small parts of 20 mm for porosity determination.

Table 1
Composition of normalised mortar

Components	Quantity
Normalised sand 0–2 mm (EN 196-1)	1350 kg
Cement CEM II/B-M 32,5 R (EN 197-1)	450 kg
Water	225 kg
Water/Cement ratio	0.5

After 6 months of immersion, samples were classified in three different series:

- protected samples from desiccation by two layers of adhesive aluminium, mentioned further as "saturated samples";
- samples submitted to desiccation in a controlled atmosphere (T=21±1 °C, Hr=45±5%), mentioned further as "desiccation samples";
- oven-dried samples at 60 °C, until constant weight and protected from resaturation by two layers of adhesive aluminium, mentioned further as "dried samples".

The experimental program is decomposed as follows (all the presented tests are performed according to the drying process and the conservation mode):

- measurements of endogenous and drying shrinkages on prisms (40×40×160 mm^3), these prisms were made up and preserved under the same previously described conditions;
- hydrostatic compression tests and triaxial compression tests on cylinders (ϕ37×74 mm);
- measurements of loss of water of prisms (40×40×160 mm) and cylinders (ϕ37×74 mm);
- measurements of porosity (ϕ37×20 mm) and permeability (ϕ37 mm×50 mm).

2.2. Experimental devices and measurements

Various tests were thus performed with this mortar: hydrostatic compression and classical triaxial compression tests with unloading–reloading cycles, permeability tests, measurements of porosity and desiccation shrinkage.

Hydrostatic compression and triaxial compression tests were carried out using a triaxial cell, a confining pump (Gilson® 307), to ensure oil injection until the required pressure level, and a hydraulic press (Instron® 500 kN capacity). A prescribed displacement mode was used, the axial strain velocity being of 2 μm s^{-1} for the deviatoric loading rate (Fig. 1a). The axial stress, applied on sample,

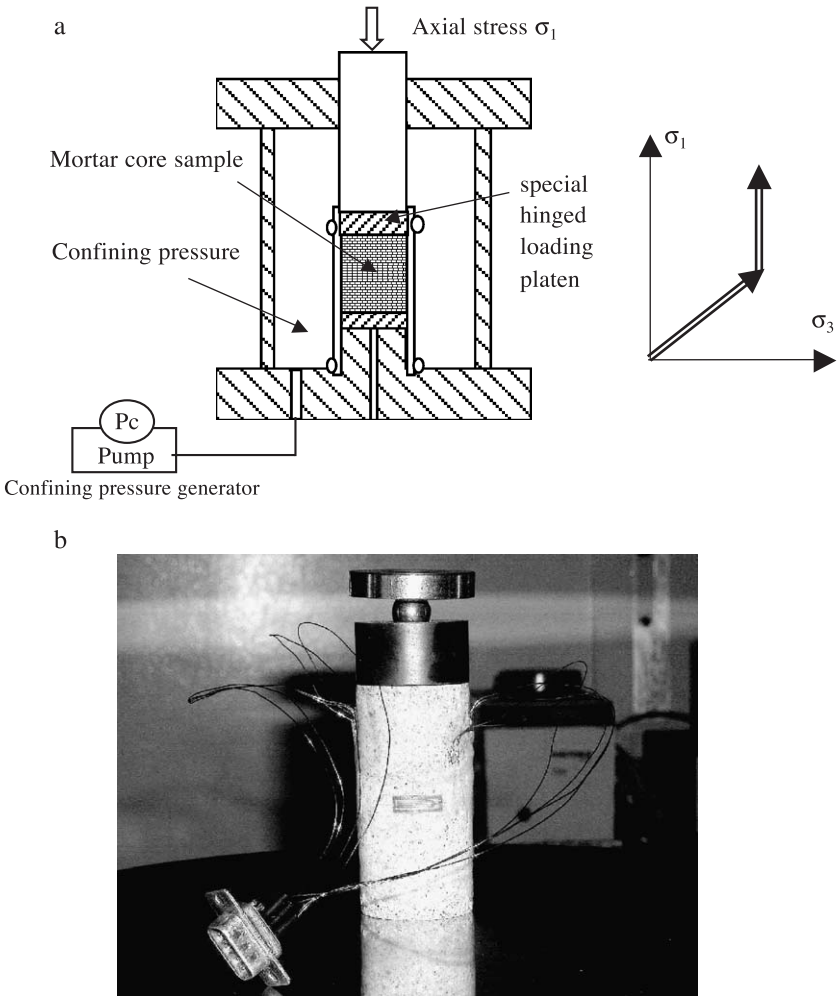

Fig. 1. (a) Principle of the triaxial compression test. (b) The special hinged loading platen and a mortar sample.

was deduced from the machine load measurement cell. The longitudinal and transversal strains were measured with four gauges: two longitudinal and two transversal, located at the middle of the sample (Fig. 1b). To carry out a perfect stress state (without significant bending effect), a special hinged loading platen was designed (Fig. 1b) and placed between the superior press platen and the sample. Imperfections due to a possible parallelism defect between the two sample surfaces were thus minimised.

The triaxial compression tests are classically conducted: loading with hydrostatic pressure until the desired level (15 MPa) and then kept constant during the deviatoric loading. The deviatoric strength is then equal to the maximum deviatoric stress reached during the test.

The characterisation of failure strength can be completed by permeability measurements, for example, as it is a key parameter among the "durability indicators". The mortar permeability was measured by ethanol injection, a liquid that is actionless with cement (for more details, see Refs. [27,28]). After 6 months in water, samples were dried up to a constant weight (at 60 °C) before testing. These permeability measures are thus affected by the effect of microcracking induced by the drying process (for example, see Refs. [27,29]). Porosity is obtained by the difference between water saturated and dried (at 60 °C) sample masses. As well as for the permeability tests, the measured porosity includes microcracks due to drying. Finally, the shrinkage measurements on prisms were achieved by a classical device (using a retractometer), corresponding to the variation of the prism length (base 160 mm).

3. Experimental results in permeability, porosity and triaxial compression

3.1. Intrinsic permeability and porosity of the normalised mortar (w/c=0.5)

To measure its permeability, the sample is subjected to a liquid flow; ethanol was chosen in the present case. The liquid permeability cell is depicted in Fig. 2. Liquid is injected at a constant pressure P_i, by a high-pressure pump (Gilson® type) from calibrated capillary tubes (3-mm diameter). Such a device has the advantage that the injected flow can be measured with a good accuracy and, as soon as a steady state flow is reached, it can be easily recorded. Furthermore, it is a direct measurement of the permeability, under steady conditions, which is carried out and based on the entry flow rate Q measurement. For such conditions, Darcy's law can be applied and leads to:

$$K_{\text{int}} = \frac{\mu Q}{S}\frac{L}{(P_i - P_0)} \tag{1}$$

where K_{int} is the intrinsic permeability (m^2), Q is the volume rate of liquid flow ($m^3 \cdot s^{-1}$) and μ the liquid viscosity

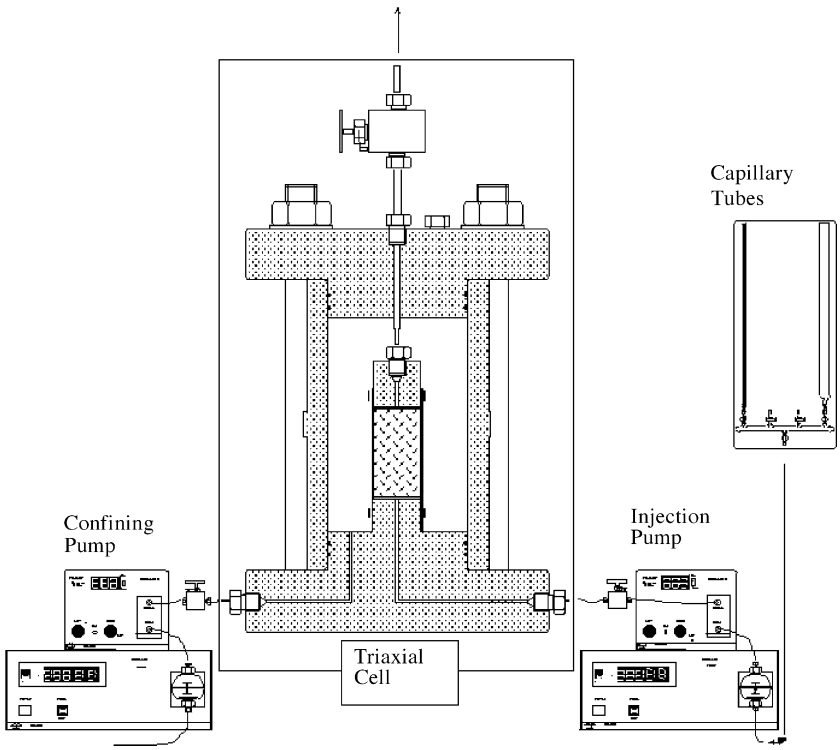

Fig. 2. Principle of the permeability measurement device.

Table 2
Values of porosity and permeability of mortar

Sample number	1	2	3	Average
Fluid permeability (10^{-17} m^2)	0.6	0.7	0.5	0.6
Porosity (%)	17.7	18.7	–	18.2

(Pa · s). P_i is maintained at 1.5 MPa during the whole test and P_0 is the atmospheric pressure as the sample is freely drained on its upper side (Pa). L and S are, respectively, the length (m) and the sample surface (m^2) of the cross-section.

Table 2 shows obtained porosity and intrinsic permeability results. The n°1 and 2 used specimens were cut in three parts: central part was used for gas permeability measurement, and others parts for porosity. The porosity, presented in Table 2, is the average of two results obtained on the slices (top and bottom of each specimen). The average permeability is equal to 0.6×10^{-17} m^2, and the average porosity 18.2%. As there is no significant scattering among these permeability values, the initial used mortar and the drying effects can be considered as homogeneous.

3.2. Desiccation shrinkage measurements

An example of drying shrinkage measurement performed on prismatic sample submitted to desiccation is depicted in Fig. 3. One can notice that endogenous shrinkage, measured on samples immerged 6 months in water and protected from desiccation, is negligible compared with drying shrinkage. This curve showing the drying shrinkage evolution versus loss of free water was obtained with retractometer measurements. The last point of this curve, denoted "dried sample" (×), corresponds to the desiccation shrinkage measured on a prismatic specimen dried at 60 °C until constant weight. The result is classical as three characteristic phases are present [30,31]: the first phase, corresponding to the weight loss with only weak shrinkage measurement, comes from rapid evaporation of surface water, coupled with an induced microcracking which counterbalances prism shrinkage; in the second phase, drying shrinkage is a linear function of loss of water; this is due to solid skeleton contraction induced by capillary depression [21,32], variation in surface energy [12] and disjoining pressure [33], (we will consider that the dominant mechanism is the capillary suction); finally, the third phase shows a weight loss evolution without additional shrinkage. The last phase can be explained either by the fact that the contraction of cement matrix becomes low by lack of free water, by a nonlinear drying and desiccation shrinkage relation, for example, due to induced microcracking, or by a nonlinear mechanical behaviour of mortar [34].

3.3. Results of hydrostatic and triaxial compression tests

For a homogeneous, elastic, linear and isotropic material, we can define classical parameters as:

$$\varepsilon_v = \frac{\Delta V}{V} = \varepsilon_1 + \varepsilon_2 + \varepsilon_3 = \frac{3(1-2v)}{E}\sigma_h = \frac{\sigma_h}{K} \tag{2}$$

where σ_h=P_c for a hydrostatic compressive test,

$$E = \frac{\sigma_1 - \sigma_3}{\varepsilon_1} \tag{3}$$

$$v = -\frac{\varepsilon_2 (= \varepsilon_3)}{\varepsilon_1} \tag{4}$$

If $\bar{\bar{\sigma}}$ represents the actual stress tensor during classical triaxial test, the hydrostatic and deviatoric components of the stress tensor can be defined as:

$$\sigma_h = \frac{(\sigma_1 + 2\sigma_3)}{3} \tag{5}$$

$$\sigma_d = \sigma_1 - \sigma_3 = \sqrt{3J_2} \tag{6}$$

where ε_1 is the axial strain, ε_2, ε_3 are the lateral strains, ε_v is the volumetric strain, E is the Young's modulus, v the Poisson's ratio, P_c the confining pressure, K the bulk modulus, σ_1 the axial stress (major stress), σ_2, σ_3 lateral stresses (minor stress), σ_h the mean stress (also named spherical stress) and σ_d is the deviatoric stress. J_2 is the second invariant of deviatoric stress tensor.

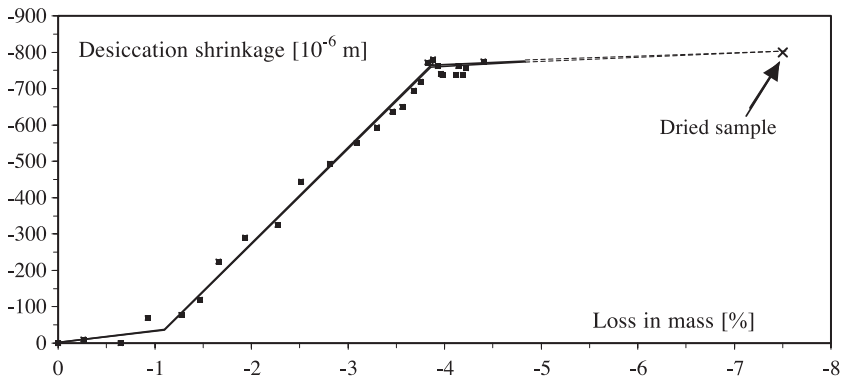

Fig. 3. Drying shrinkage versus loss in mass for normalised mortar.

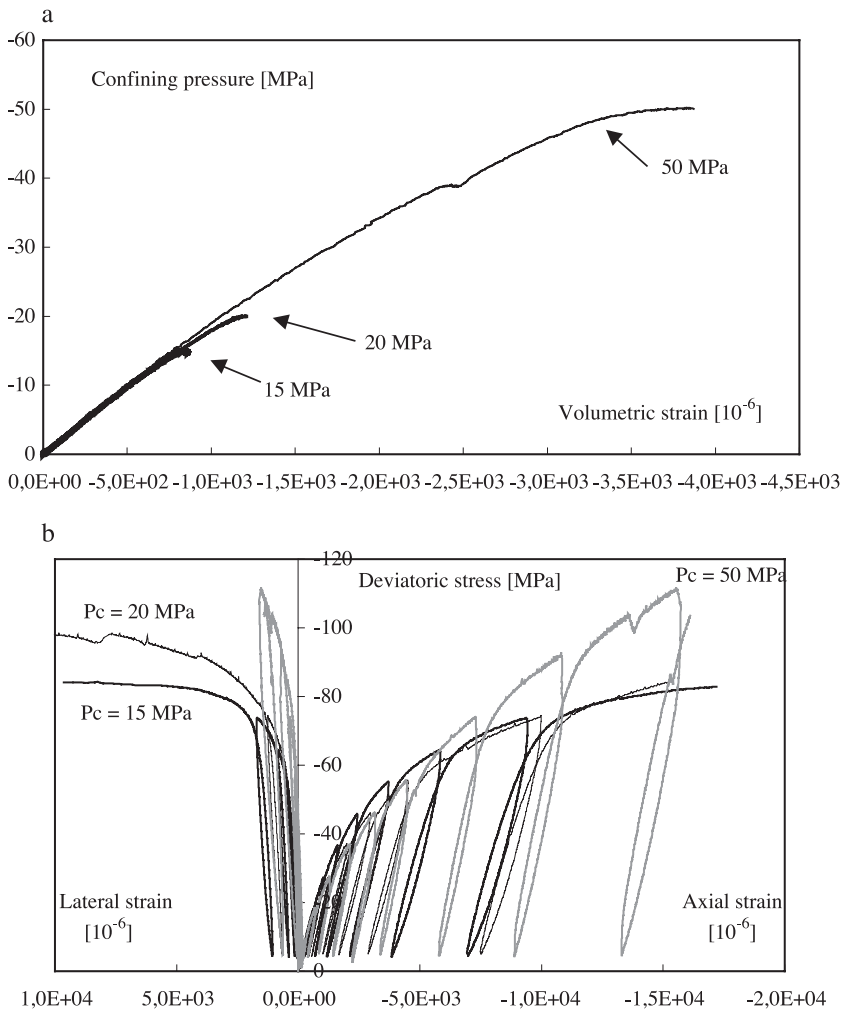

Fig. 4. (a)Variation of the volumetric strain versus the confining pressure in hydrostatic test. (b) Deviatoric stress versus axial and lateral strains for different confining pressure (15, 20 and 50 MPa).

Obtained results from triaxial compression tests are presented on Figs. 4a and b. Fig. 4a displays the variation of volumetric strain (ε_v) versus the applied confining pressure (P_c), while the variations of axial strain (ε_1) and lateral strains (ε_2=ε_3) versus deviatoric stress ($\sigma_1-\sigma_3$) are plotted Fig. 4b. The strain values reported there were calculated by averaging the two corresponding gauge measurements, as preliminary tests showed they were virtually identical either for hydrostatic or triaxial compression tests. Due to the measurement device, the axial strains are limited to about $16{,}000\times10^{-6}$. Rupture of specimens was obtained under low confining pressure (15 and 20 MPa), whereas failure strength was not reached under 50 MPa of confinement. Measurements of initial Young's modulus (Eq. 3) and Poisson ratio (Eq. 4), as well as their variations with mechanical loading, were also processed. Young's modulus measurements were conducted following RILEM recommendations [35], extended to the case of triaxial compression as being the secant modulus measured after three loading–unloading cycles up to a 9-MPa maximal deviatoric stress and the initial Poisson ratio being minus the ratio between the lateral deformation reached after these three cycles divided by axial deformation at the same stage. Variations in elastic modulus and Poisson ratio can therefore be evaluated according to the maximal deviatoric stress value. The bulk modulus can be determined by two different ways: direct determination from hydrostatic compression test or by using Eq. (2), with material elastic parameters deduced from triaxial compression test. The second method allows, by comparison of both results, to verify the reliability of elastic parameters measurements. To maximise measurement accuracy on Young's modulus and Poisson's ratio, each material behaviour was meticulously analysed. This measurement process was performed on each specimen. Material behaviour exhibits hysteretic loops, which are due to material viscosity [36]. One can notice that their opening decreases with drying. Obtained results according to mechanical damage in multiaxial compression test are very similar with those presented in the literature on this classical mortar.

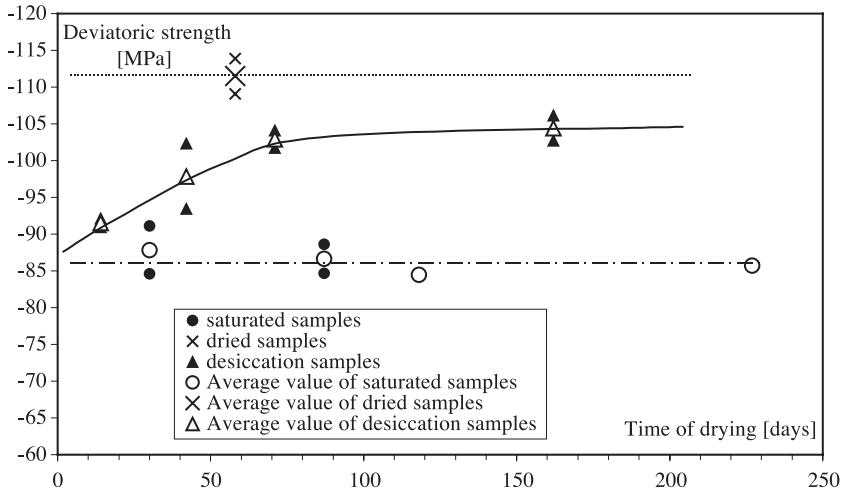

Fig. 5. Deviatoric strength versus time of drying.

Besides, the behaviour of tested mortar in triaxial compression evolves between a brittle behaviour (15 and 20 MPa of confining pressure) toward a ductile behaviour (P_c=50 MPa). As the main objective was to evaluate the influence of the drying induced microcracking on the multiaxial mechanical behaviour of a mortar, it was hence decided to perform primary several tests with a confining pressure equal to 15 MPa, to emphasize the microcracking phenomenon on the material failure process.

3.3.1. Triaxial compression strength evolution (P_c=15 MPa)

Triaxial compression results can be analysed in relation to the drying time of mortar. For each considered time of drying, two cyclic triaxial compression tests were carried out on the same day. Finally, two dried samples were tested with the purpose to simulate complete drying, that is, no more free water into the material.

Authors showed that the desiccation increased the strength of cementitious materials [10,11,37–39] and decreased the mortar's elastic characteristics under uniaxial compression [37,38]. Results of triaxial compression tests according to the drying time (Fig. 5) clearly display the effect of desiccation on the maximal deviatoric strength: an increase of about 29% (this increase was about 21% for uniaxial compression strength [37,38]) from the value obtained for saturated samples to those obtained on dried specimens. To verify that no maturation effect occurs during the experimental campaign, the tests on samples preserved from desiccation (point ●) were made periodically. In Fig. 5, time t = 0 corresponds to the beginning of the drying. The dried specimens (point ×) exhibit a higher strength compared with the samples protected from desiccation, whereas specimens left in the natural desiccation (point ▲) have a deviatoric strength which evolves, during drying, from saturated sample values towards dried sample values of strength.

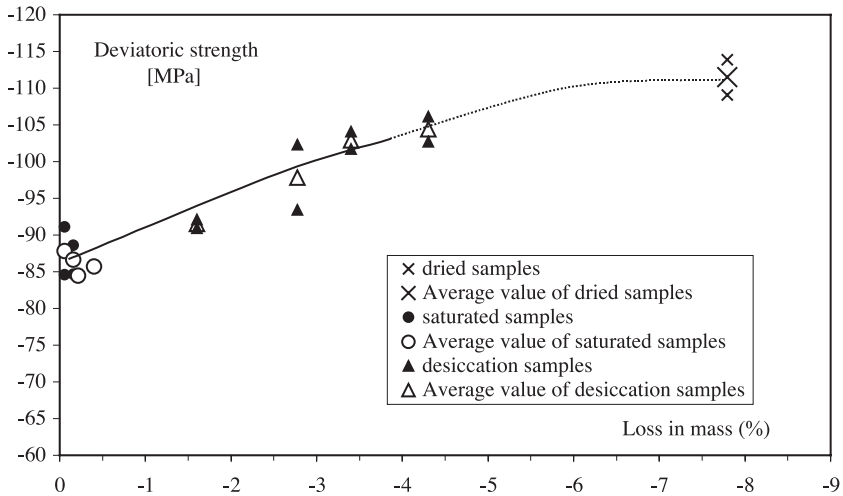

Fig. 6. Deviatoric strength versus loss in mass.

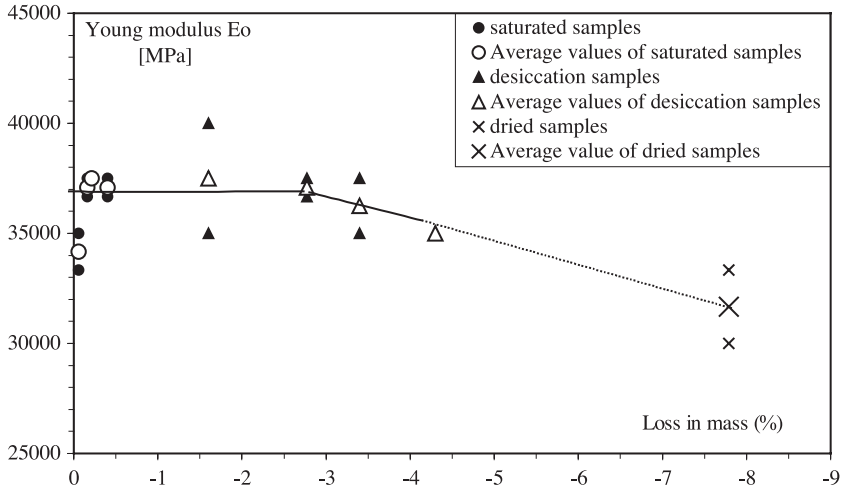

Fig. 7. Young's modulus versus loss in mass.

The same tendency is observed on Fig. 6, where the evolution of the mortar deviatoric strength is plotted versus the mass loss. The failure deviatoric strength of desiccation samples (▲) increase with mass loss to finally reach that of the dried samples (×). One can notice that desiccation samples do not reach the strength of dried samples, which was not the case when measured in uniaxial compression [37,38]. This comes from an amount of free water evaporated, from specimens during natural desiccation, smaller than for dried samples at 60°C. Therefore, the lower the suction effect is, the lower the increase of deviatoric strength will be.

Besides the effect of confining pressure, the mortars' deviatoric strength increase can be attributed to two concomitant phenomena. The first is the capillary suction effect, leading to a compression of the solid skeleton, similar to a "prestressing" of mortar, which will be, as a result, more resistant. This phenomenon was often mentioned for rocks [40]. Thus, there will be an increase of the triaxial compression strength, with hydrous pressure gradient or not. This capillary suction can be considered as isotropic; this could partially justify the more important strength increase (29%) observed under multiaxial compression loading (the suction is "active" in a multiaxial way), compared with uniaxial compression (21%). The second phenomenon is linked to the moisture gradients, present in the sample during drying. The induced contraction of the external part of the sample leads, first, to a microcracking and also to a confining effect on the "non-retracting" central part [10,21]. This phenomenon, obviously observed for the desiccation sample, brings about an overconfining effect, which is not to be active for the oven-dried sample of uniform humidity content. Moreover, when these low permeability samples are tested closed to complete saturation, the mean compressive stress increase may induce an interstitial overpressure known as the Skempton effect (under undrained conditions [41,42]). This effect would amplify the opening and propagation of microcracks previously induced by drying.

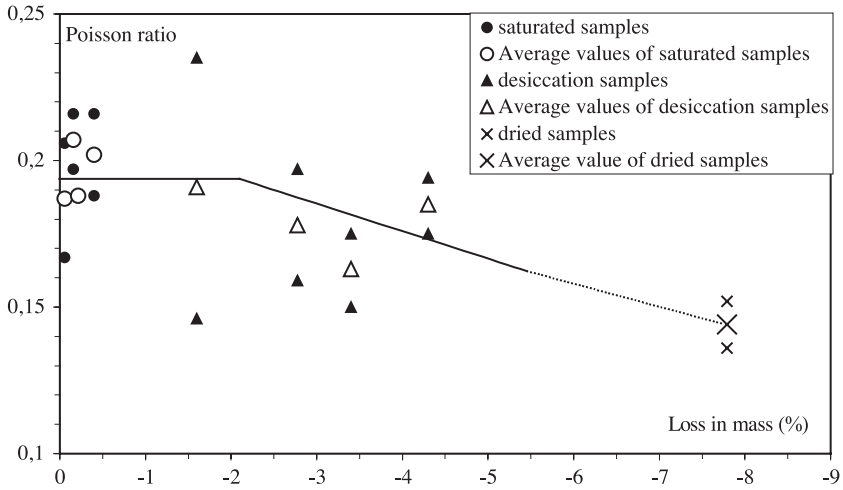

Fig. 8. Poisson's ratio versus loss in mass.

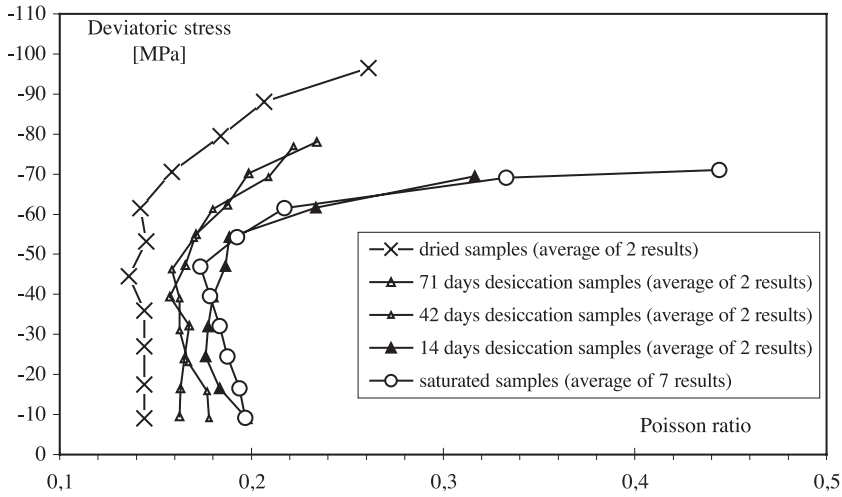

Fig. 9. Variation of deviatoric stress versus Poisson's ratio.

On the other hand, strength increase under triaxial compression (29%) is higher than the increase of uniaxial compression strength (21%) during complete drying. This phenomenon may be due to the fact that interstitial pressure is initially higher in the triaxial case. Hence, induced microcracking, which plays an important role in failure process, would be more pronounced under deviatoric loading, when the sample is close to complete saturation. When failure occurs, it can be observed that macrocracks and shearing band divide the sample into two or three parts. Under low confining pressure conditions, this type of failure is frequently reported in the literature [1–7,9].

3.3.2. Measurements of Young's modulus and Poisson's ratio under triaxial loading–drying effect

Young's modulus and Poisson's ratio evolutions, versus loss in mass during drying, are respectively plotted on Figs. 7 and 8. Both Young's modulus and Poisson's ratio vary between two limit values: an upper one (that of saturated samples) and a lower one (that of dried samples). Inside this range, Young's modulus value of desiccation samples remains constant in the first stage, before an almost 15% decrease to eventually reach the dried sample values. Poisson's ratio variations are quite similar, with a decrease around 25%. The loss in mass threshold, from which elastic parameters begin their drop, is in the range of 2.5–3% (about 40 drying days).

Two different effects can be attributed to hydrous gradient, as they are coming along with increase of capillary suction: microcracking (induced by desiccation) and the previously mentioned structural effect, causing mortar sample prestressing. From the latter, the measured Young's modulus can be considered as an apparent stiffness. One can mention there that under intermediate saturation state, the humidity content cannot be considered to be uniform through the sample. As a possible structural effect is thus possible, elastic property measurements and strength determinations have to be carefully used for numerical analysis.

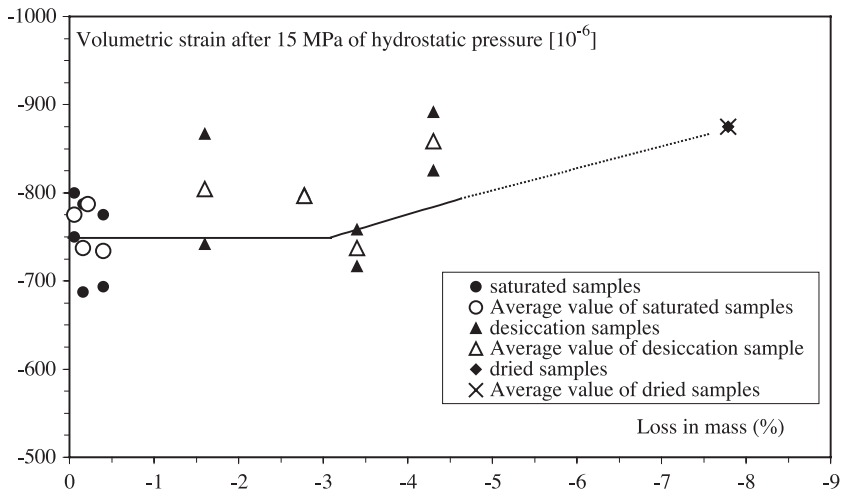

Fig. 10. Volumetric strain (after 15 MPa of hydrostatic pressure) versus loss in mass.

Microfissuration involved with drying must logically cause a Young's modulus decrease; this assertion is thus consistent with the final values of the latter for desiccation samples and the decrease of elastic stiffness observed after a significant amount of lost free water. The loss in mass threshold, from which elastic parameters begin to decrease, is also the state from which no more drying shrinkage is observed (phase 3; Fig. 3). At this stage, the sample prestressing should not counterbalance the microcracking growing, leading hereby to visible hydrous damage phenomena.

The variations in Poisson's ratio versus maximal deviatoric stress, that is the higher value of applied stress for each loading–unloading cycle, are presented Fig. 9 for the three types of samples. For low stress value, Poisson ratio remains almost constant up to a 54 MPa value for saturated samples and 62 MPa value for dried samples. Beyond these values, there is a sharp increase of these ratios, which is nevertheless smoother for dried samples. The lower stress value, 54 MPa face to 62 MPa, could be attributed to the interstitial pressure and its effect on the microcracks opening. The desiccation samples behaviour is intermediate when compared with the limit cases (dried or saturated). Furthermore, the threshold stress value from which Poisson's ratio is varying sharply seems to increase with drying time, even if there is no obvious difference between 42 and 71 days. It is somewhat difficult, in such a case, to clearly distinguish what is due to structural effect or to a possible poromechanical coupling, and its outcome upon microcracks opening.

3.3.3. Drying effects on volumetric strain and compressibility

Volumetric strain versus loss in mass, depicted in Fig. 10, concerns samples under hydrostatic loading up to 15 MPa, that is, the stress level reached before axial loading in triaxial compression test. At the same level of hydrostatic pressure, an increase in volumetric strain of about 15% can be observed from the saturated to dried samples. This

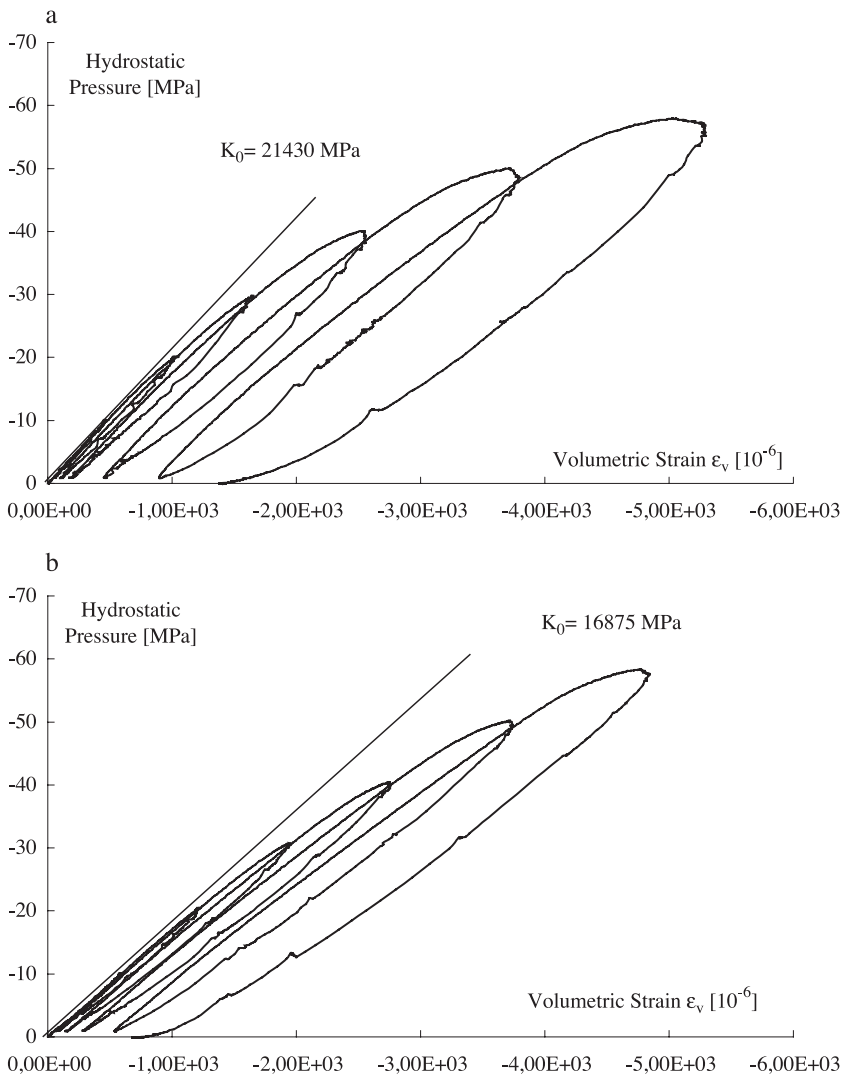

Fig. 11. (a) Hydrostatic pressure versus volumetric strain for a saturated sample. (b) Hydrostatic pressure versus volumetric strain for a desiccation sample (loss in mass 4.3%). (c) Hydrostatic pressure versus volumetric strain for a dried sample. (d) Hydrostatic pressure versus strain for each guage measured on a desiccation sample.

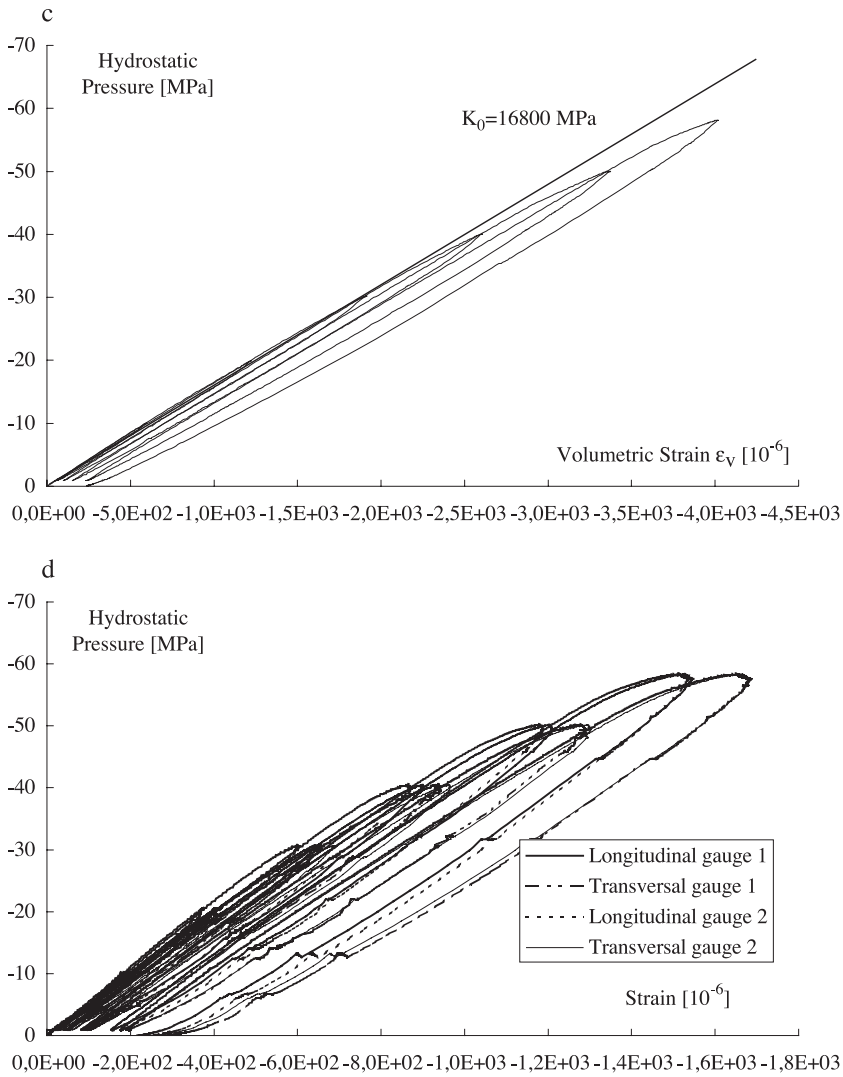

Fig. 11 (*continued*).

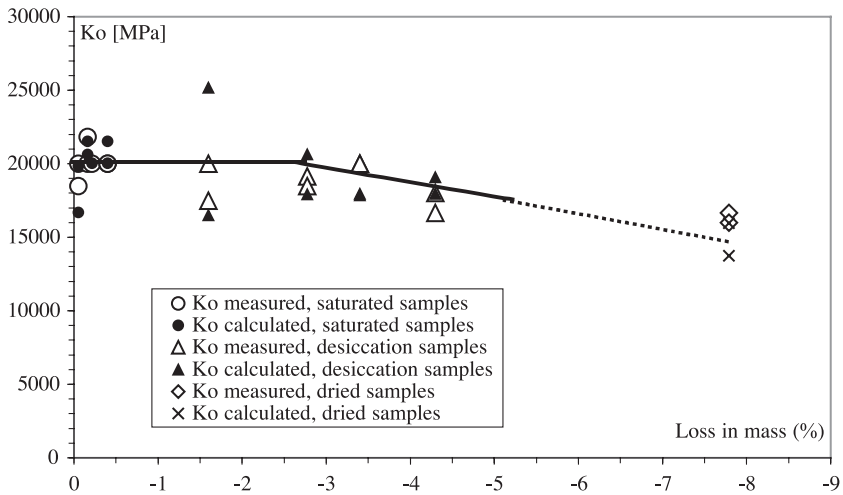

Fig. 12. Variation of initial bulk modulus (K_0) versus loss in mass.

increase may be attributed to an affective stress effect, that is transition from undrained to drained behaviour. Another part of this increase comes from the microcracks closure; such an impression is confirmed by Fig. 11a–c, showing the test results on samples preserved under different conditions, the highest value of hydrostatic pressure now being of 60 MPa. On a general case, during a hydrostatic loading, it is observed that an initial elastic behaviour is followed by plastic deformations and a collapse or a consolidation; at this stage, the behaviour can be assumed to be elastic-plastic. When loading is growing up, stiffening is often observed [24,36]. The strain gauge responses lead us to assume that, in a first approximation, the behaviour remains isotropic (Fig. 11d), which, thus, is an evidence of a diffuse and not orientated microcracking due to hydrous damage. The residual strain, coming from elastic-plastic behaviour, is higher in the case of saturated sample. In fact, after a longer drying time, the material behaviour becomes more damageable; as a result, under hydrostatic loading, a decrease of the bulk modulus and fewer plastic residual strains are to be observed (Fig. 11c). Thus, the multiaxial mechanical behaviour is varying from elastic-plastic to damageable elastic-plastic when free water evaporates from material. Such a phenomenon was also put in evidence on concrete under uniaxial compressive loading [32,38].

Variations of isotropic modulus K versus loss in mass were measured during the first hydrostatic phase of triaxial loading, that is, to a final level of 15 MPa. These variations are presented on Fig. 12 and would be similar to those obtained, by calculation (Eq. 2), with the elastic parameters deduced from triaxial tests (Figs. 7 and 8). As a partial conclusion, one can say that hydrous damage coming from desiccation will induce diffuse microcracking, leading to multiaxial elastic property diminution.

4. Conclusions

This experimental study has put in light the influence of drying and desiccation shrinkage on mechanical behaviour of a normalised mortar submitted to triaxial compressive loading. An increase of mortar deviatoric strength (29%) is undoubtedly linked to the desiccation, while, for elastic parameters, a contrary variation is observed. The Young's modulus and Poisson's ratio decrease was respectively about 15% and 25% for the studied mortar, from saturated to dried conditions. These opposite phenomena come not only from capillary depression generated by drying, but also from the microcracking induced by the differential contraction between the external and internal parts of the samples and by the presence of aggregates. A drying damage is then obtained without any mechanical loading. Such a drying effect has to be involved in modelling the coupling effect of desiccation as regards to the mechanical behaviour of concrete. Another desiccation effect is also observed: a transition from elastic-plastic to damageable elastic-plastic behaviours as drying is processing. Because of an initial balance between capillary suction and microcracking evolution effects, the decrease of elastic properties is observed after 2.5–3% loss in mass only. It is of interest to emphasize there, that these 2.5–3% loss in mass is close to the threshold, beyond which, no more desiccation shrinkage is measured during drying. At this stage, another question can be raised: are the elastic property decreases able to induce a part of the concrete Pickett effect (see in general Ref. [43]), observed under creep with desiccation? Such a hypothesis needs complementary tests to be performed and will be the purpose of further studies.

References

[1] D. Sfer, I. Carol, R. Gettu, G. Etse, Study of the behaviour of concrete under triaxial compression, ASCE J. Eng. Mech. 128 (2) (2002) 156–163.
[2] R. Palaniswamy, S.P. Shah, Deformation and failure of hardened cement paste subjected to multiaxial stresses, The Deformations and the Rupture of Solids Subjected to Multiaxial Stresses, Proc. of RILEM Int. Symposium, RILEM, Paris, 1972, pp. 169–179.
[3] R. Palaniswamy, S.P. Shah, Fracture and stress–strain relationship of concrete under triaxial compression, J. Struct. Div., ASCE, ST5 (1974) 901–916.
[4] The Deformations and the Rupture of Solids Subjected to Multiaxial Stresses, Proc. of RILEM Int. Symposium, Cannes, RILEM, Paris (1972).
[5] C.A. Rutland, M.L. Wang, The effects of confinement on the failure orientation in cementious materials: experimental observations, Cem. Concr. Compos. 19 (2) (1997) 149–160.
[6] R.G. Zimmerman, Major factors affecting the multiaxial compressive strength of plain concrete, The Deformations and the Rupture of Solids Subjected to Multiaxial Stresses, Proc. of RILEM Int. Symposium, Cannes, RILEM, Paris, 1972, pp. 257–272.
[7] R. Bellotti, P. Rossi, Cylinder tests: experimental technique and results, Mat. Struct. 24 (1991) 45–51.
[8] H. Meziani, F. Skoczylas, An experimental study of the mechanical behaviour of a mortar and its permeability under deviatoric loading, Mat. Struct. 32 (1999) 403–409.
[9] J.G.M. van Mier, Strain softening of concrete under multiaxial loading conditions, Doctoral Dissertation, Eindhoven University of Technology, The Netherlands (1984).
[10] F.M. Bartlett, J.G. MacGregor, Effect of moisture condition on concrete core strengths, ACI Mater. J. 91 (3) (1994) 227–236.
[11] S. Popovics, Effect of curing method and moisture condition on compressive strength of concrete, ACI Journal 83 (4) (1986) 650–657.
[12] F.H. Wittmann, Creep and shrinkage mechanisms, in: Z.P. Bažant, F.H. Wittmann (Eds.), Creep and Shrinkage in Concrete Structures, Wiley, Chichester, 1982, pp. 129–161.
[13] P. Jamet, A. Millard, G. Nahas, Triaxial behaviour of a micro-concrete complete stress-strain for confining pressures ranging from 0 to 100 MPa, Proc. of International Conference on Concrete under Multiaxial Conditions, vol. 1, Presses de l'Université Paul Sabatier, Toulouse, 1984, pp. 133–140.
[14] Z.P. Bažant, W.J. Raftshöl, Effect of cracking in drying and shrinkage specimens, Cem. Concr. Res. 12 (1982) 209–226.
[15] H. Sadouki, F.H. Wittmann, Shrinkage and internal damage induced by drying and endogeneous drying, in: V. Baroghel-Bouny, P.-C. Aïtcin (Eds.), Shrinkage of Concrete, RILEM Publications PRO 17, Paris, France, 2000, pp. 299–314.
[16] N. Hearn, Effect of shrinkage and load-induced cracking on water permeability of concrete, ACI Mater. J. 96 (2) (1999) 234–241.

[17] J. Bisschop, J.G.M. van Mier, Meso-level mechanisms of drying shrinkage cracking in concrete. Proc. of Int. RILEM Workshop on Fracture and Durability, Post-Conference Workshop of Framcos IV, June 1st, Cachan, France (2001).
[18] J. Bisschop, L. Pel, J.G.M. van Mier, Effect of aggregate size and paste volume on drying shrinkage microcracking in cement-based composites, in: F.-J. Ulm, Z.P. Bažant, F.H. Wittmann (Eds.), Creep, Shrinkage and Durability Mechanics of Concrete and other Quasi-Brittle Materials, Elsevier, 2001, pp. 75–80.
[19] J. Bisschop, J.G.M. van Mier, How to study drying shrinkage microcracking in cement-based materials using optical and scanning electron microscopy? Cem. Concr. Res. 32 (2002) 279–287.
[20] H. Colina, P. Acker, Drying cracks: Kinematics and scale laws, Mat. Struct. 33 (2000) 101–107.
[21] P. Acker, Comportement mécanique du béton : apport de l'approche physico-chimique, Thèse de doctorat de l'Ecole Nationale des Ponts et Chaussées, Paris, Rapport de Recherche LPC n°152 (1988) (in French).
[22] H.W. Reinhardt, Relation between the microstructure and structural performance of concrete, in: A. Aguado, R. Gettu, S.P. Shah (Eds.), Technology Transfer on the New Trend in Concrete, Proc. of Con-Tech'94, Barcelona, RILEM, Paris, 1994, pp. 19–32.
[23] A.M. Neville, Properties of Concrete, 4th ed., Longman Group, 1995.
[24] N. Burlion, G. Pijaudier-Cabot, N. Dahan, Experimental analysis of compaction of concrete and mortar, Int. J. Numer. Anal. Methods in Geomech. 25 (2001) 1467–1486.
[25] P.-C. Aïtcin, A. Neville, P. Acker, Les différents types de retrait du béton, Bull. Lab. Ponts Chaussées 215 (ref. 4184) (1998) 41–51 (in French).
[26] G.J. Verbeck, Carbonation of hydrated Portland cement, ASTM. Spec. Tech. Publ. 205 (1958) 17–36.
[27] N. Burlion, F. Skoczylas, Gas permeability tests on concrete damaged by drying shrinkage and its anisotropy effect, in: R. de Borst, J. Mazars, G. Pijaudier-Cabot, J. van Mier (Eds.), Fracture Mechanics of Concrete and Concrete Structures, Proc. of Int. Conf. FRAMCOS-4, Cachan, France, RILEM, Paris, 2001, pp. 333–340.
[28] H. Loosveldt, Z. Lafhaj, F. Skoczylas, Experimental study of gas and liquid permeability of a mortar, Cem. Concr. Res. 32 (9) (2002) 1357–1363.
[29] N. Burlion, F. Skoczylas, T. Dubois, Induced anisotropic permeability due to drying of concrete, Cem. Concr. Res. 33 (5) (2003) 679–687.
[30] J.-M. Torrenti, L. Granger, M. Diruy, P. Genin, Modélisation du retrait du béton en ambiance variable, Revue Française de Génie Civil 1 (4) (1997) 687–698 (in French).
[31] L. Granger, Comportement différé du béton dans les enceintes de centrales nucléaires : analyse et modélisation, Thèse de doctorat de l'Ecole Nationale des Ponts et Chaussées, Paris (1994) (in French).
[32] N. Burlion, F. Bourgeois, J.F. Shao, Coupling damage-drying shrinkage : experimental study and modelling, in: V. Baroghel-Bouny, P.-C. Aïtcin (Eds.), Shrinkage of Concrete, RILEM Publications PRO 17, Paris, France, 2000, pp. 315–339.
[33] Z.P. Bažant, F.H. Wittmann, Creep and Shrinkage in Concrete Structures, Wiley, Chichester, 1982.
[34] F. Meftah, J.-M. Torrenti, W. Nechnech, F. Bendoudjema, C. de Sa, An elasto-plastic damage approach for the modelling of concrete submitted to the mechanical induced effects of drying, in: V. Baroghel-Bouny, P.-C. Aïtcin (Eds.), Shrinkage of Concrete, RILEM Publications PRO 17, Paris, France, 2000, pp. 341–354.
[35] RILEM TC14-CPC, Modulus of elasticity of concrete in compression (CPC8), Mat. Struct. 6 (30).
[36] J. Mazars, Mécanismes physiques de rupture et modèles de comportement mécanique du béton hydraulique, Béton Hydraulique : Connaissance et Pratique, Presses de l'Ecole Nationale des Ponts et Chaussées, 1982, pp. 295–316 (in French).
[37] I. Yurtdas, N. Burlion, F. Skoczylas, Experimental characterisation of the drying effect on uniaxial mechanical behaviour of mortar, Mat. Struct. (in press).
[38] N. Burlion, I. Yurtdas, F. Skoczylas, Comportement mécanique et séchage de matériaux à matrice cimentaire : comparaison mortier-béton, Revue Française de Génie Civil 7 (2) (2003) 145–165 (in French).
[39] H.J. Gilkey, The moist curing of concrete, Eng. News-Rec. 119 (1937) 630–633.
[40] S. Jumikis, R. Alfreds, Rocks Mechanics, 2nd ed., Trans Tech Publications, Clausthal-Zellerfeld, 1983.
[41] O. Coussy, Mechanics of porous continua, Wiley, Chichester, 1995.
[42] J.R. Rice, M.R. Cleary, Some basic stress-diffusion solutions for fluid-saturated elastic porous media with compressible constituents, Rev. Geophys. 14 (1976) 227–241.
[43] F.-J. Ulm, Z.P. Bažant, F.H. Wittmann, Creep, Shrinkage and Durability mechanics of Concrete and other Quasi-Brittle Materials, Elsevier, 2001.